ULTRA-WIDE BANDWIDTH, LOW VOLTAGE, AND CHIRP-FREE OPTICAL INTENSITY MODULATOR: DESIGN AND PERFORMANCE ANALYSIS

M.T.Camargo Silva and C.A.De Francisco

Optoelectronics and Systems Research Laboratory
University of São Paulo - 13560-250 Sao Carlos SP Brazil

ABSTRACT

A novel wavelength-selective InGaAs/InP coupled asymmetric quantum well electrorefraction type optical intensity modulator is proposed. The device is based on contradirectional exchange Bragg grating coupled-waveguide structure, which avoids the use of an interferometer. For a non-optimized device the bandwidth is 111 GHz at 1.67 V and it is chirp-free. The device can be integrated with lasers, optical amplifiers, photodetectors etc. It can also be integrated in tandem.

INTRODUCTION

High bit rate and long-haul wavelength division multiplexing (WDM) lightwave communication systems have prompted investigations on external intensity modulation schemes. The goal is to eliminate the wavelength chirping arising in high-speed directly modulated lasers which limits the span-rate system product. For electrorefraction (ER) type intensity modulators the main design trade-off is to achieve maximum refractive index change and minimum absorption loss. It has been shown [1], that in uncoupled multiquantum well (UMQW) structures large refractive index change is obtained at wavelengths close to the excitonic resonance due to the quantum confined Stark effect (QCSE). However, for small insertion loss the operation wavelength must be set far below the exciton peak where the refractive index change has decreased considerably. This feature associated to the QCSE induced electroabsorption narrows the bandwidth, increases the voltage, and decreases the chirping parameter. As an alternative, it has been theoretically shown [2] that in InGaAs/InP coupled asymmetric quantum wells (CAQW) structures large negative refractive index change, at very low electric field, is achieved at wavelengths close to the absorption edge with small loss, which is due to the excitonic effects in the coupled quantum wells. In addition, CAQW presents negligible QCSE which makes the modulator chirp-free. Unfortunately, the traditional design of ER intensity modulator is inconvenient due to the requirement of an interferometric configuration and the devices are longer than the electroabsorption (EA) modulators. Also, it must be highlighted that neither the electroabsorption nor the interferometric electrorefraction modulators can be integrated in tandem, e.g. for compact multiplexers, since they are not wavelength-selective devices.

In this paper, we present the design and performance analysis of a wavelength-selective InGaAs/InP CAQW electrorefraction type optical intensity modulator operating at 1.55 μm. The device is based on a contradirectional exchange Bragg grating coupled-waveguide structure, which avoids the use of an interferometer. For a non-optimized device the bandwidth is 111 GHz at 1.67 V and it is chirp-free.

DEVICE STRUCTURE AND OPERATION

The device is shown schematically in Figure 1. The lower waveguide core is constituted of $1x10^{17}$ cm^{-3} N-doped InGaAsP, refractive index $n_1 = 3.1700$, of thickness $d_1 = 0.9$ μm. The upper waveguide core with thickness $(d_2 + g/2) = 0.925$ μm and refractive index $n_2 = 3.2572$, is comprised of m ($10 \leq m \leq 20$) periods of intrinsic, $1x10^{14}$ cm^{-3} N-doped, coupled wells with thickness a and of $6x10^{17}$ cm^{-3} N-doped and $1x10^{17}$ cm^{-3} P-doped InGaAsP layers of thickness $b = [d_2 - (t + a)]/2$. The quantum well period consists of two InGaAs asymmetric wells, 40 Å and 30 Å thick, coupled through a 50 Å thick InP barrier. The periods

WE 3F

0-7803-3246-6/96/$5.00 © IEEE

are uncoupled from each other by 100 Å InP barrier. In the active section of length L_a the InGaAsP layer is etched to a depth t. The grating with period Λ and depth g = 0.15 μm is patterned on the reflector sections of length L_g. The waveguide cores are enclosed by $1x10^{17}$ cm^{-3} N and P-doped InP, refractive index $n_3 = 3.1495$. The waveguide cores are separated by a $1x10^{17}$ cm^{-3} N-doped InP layer of thickness s = 0.4 μm. P^+ InGaAs topped the device. Ohmic contacts for modulation and ground electrodes are provided on top of the active section and on bottom of the N^+ InP substrate.

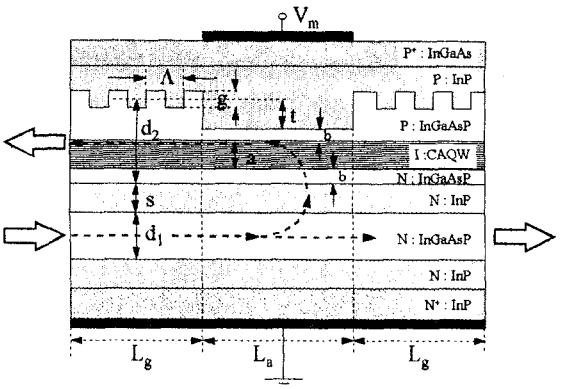

Figure 1. Modulator longitudinal cross section

In the absence of the modulation voltage V_m, the two Bragg reflectors are π/2 phase-shifted relative to each other at the operating wavelength and the device becomes a transmission resonator. Light coupled to the device through the lower waveguide input port will be transmitted to the output port of this guide. The application of the modulation voltage induces a refractive index change due to the excitonic effects in the upper waveguide core CAQW layer of the active section, yielding a phase-shift in this region and the light is exchange Bragg coupled contradirectionally into upper guide output port. Therefore, this device can be utilized as a wavelength-selective optical intensity modulator.

MODULATOR DESIGN

The device is composed of an exchange Bragg directional coupler consisting of two asymmetric planar waveguides close to each other as depicted in Figure 1. It is assumed that the antisymmetric composite mode is excited in the input waveguide. Afterwards, this forward antisymmetric mode will couple with the backward symmetric mode propagating in the output guide through the exchange Bragg.

The upper waveguide core comprises the CAQW and the InGaAsP layers. These two layers have the same refractive index through suitable selection of InGaAsP composition. In our design the InGaAsP layers were introduced for two purposes, grating fabrication and enhancement of the well confinement factor.

To compute the propagation constants of the modes, the coupled-mode equations [3,4] with suitable modifications to include the material absorption of the five-layers structure were numerically solved. The grating period, Λ, was determined from the phase-matching condition $\Lambda = 2\pi/(\beta_s + \beta_a)$, where β_s and β_a are the propagation constants of the symmetric and antisymmetric modes.

The InP and InGaAsP refractive indices were taken from reported data [5] and the CAQW refractive index was estimated from that of InGaAsP having the same bandgap. The intrinsic absorption loss of N and P-doped InP and InGaAsP were estimated from published data [6,7]. The CAQW absorption coefficient [2] at 1.55 μm is small 5 cm^{-1}. The refractive index change at 1.55 μm as a function of the applied electric field for the 30Å/40Å InGaAs CAQW with 50Å InP barrier was obtained by fitting the data provided [2]. For an electric field of ~ 35 KV/cm the refractive index change of ~ - $7.5x10^{-3}$ is achieved. Therefore, an electric field of ~ 35 KV/cm was set in our device to obtain maximum refractive index change.

The electric field distribution of the symmetric and antisymmetric modes of the structure is shown in Figure 2. As can be seen in the figure, the electric field strength of both modes are large in the upper border of the output waveguide where the grating is located. Since the grating coupling coefficient is proportional to the electric field strength of the modes, the placement of the waveguides relative to each other is an important parameter to be considered. For this purpose the waveguide separation distance was set at s = 0.4 μm.

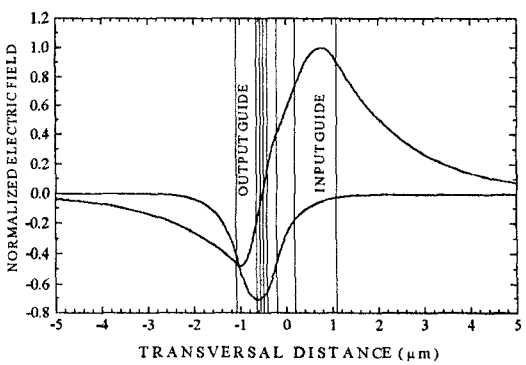

Figure 2. Electric field distribution of the symmetric and antisymmetric modes of the structure.

The symmetric mode well confinement factor is an significant parameter in device performance since the excitonic effect induced phase-shift is proportional to it.

It can be observed in the figure that with no applied voltage light transmission at the operating wavelength occurs. The insertion loss of the modulator is 3.0 dB. The application of 1.67 V to the device results in high attenuation, 23.0 dB, of the light due to the excitonic effect induced phase-shift in the active region of the modulator and the light is exchange Bragg coupled contradirectionally into upper guide output port. The device extinction ratio is 20.0 dB. The width of the stop-band is only 30 Å. In this simulation $KL_g = 1.55$, yielding a reflector length $L_g = 268$ μm. The active length is $L_a = 96$ μm. The device length is 632 μm.

The device bandwidth, extinction ratio, and applied voltage as a function of the number of periods of CAQW is shown in Figure 5. For these simulations a waveguide 2 μm wide was considered, the active region etched depth is t = 0.3 μm, and $KL_g = 1.65$.

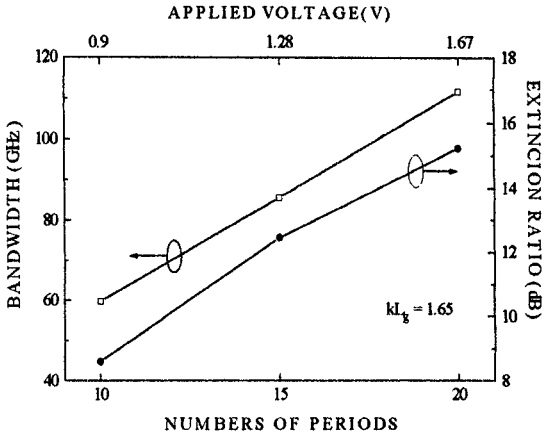

Figure 5. Device bandwidth, extinction ratio, and applied voltage as a function of the number of periods of CAQW.

As can be observed in the figure, increasing the number of CAQW periods the bandwidth, extinction ratio, and voltage increase. The increased extinction ratio is related to increasing CAQW excitonic effect induced phase-shift in the active region. As the phase-shift increases the active region length decreases. This feature associated to thicker intrinsic region decreases the capacitance and as a result increases the bandwidth. Device bandwidth as wide as 111 GHz at 1.67 V with 15 dB of extinction ratio can be achieved with an insertion loss of only 3.18 dB and length of 630 μm.

The device active region, total length, and bandwidth as a function of the active region depth is shown in Figure 6. Increasing the depth of the active region the difference of the propagation constants in the active and reflector regions also increases, resulting in larger phase-shift in the active region. To keep the phase-shift constant the active region length must be decreased. Smaller active

The well confinement factor as a function of the number of CAQW periods was also simulated and the results are shown in Figure 3.

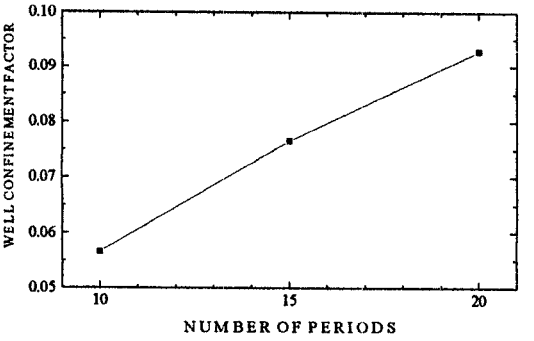

Figure 3. Symmetric mode well confinement factor as a function of the number of the CAQW periods.

The well confinement factor increases substantially with the number of periods and reaches 9.3% for 20 periods as shown in the figure.

PERFORMANCE ANALYSIS

To investigate the performance of the device, studies in relation to extinction ratio, insertion loss, and electrical bandwidth were carried out. The extinction ratio and insertion loss of the device were achieved from the power transmission spectrum at specific conditions of device geometry and applied voltage.

The power transmission spectra of a device with no applied voltage and with the application of 1.67 V is shown in Figure 4. The device parameters are 20 CAQW periods a = 0.44 μm, active region etched depth t = 0.2 μm, grating period Λ = 0.2415 μm, and grating coupling coefficient $K = 57.7\ cm^{-1}$.

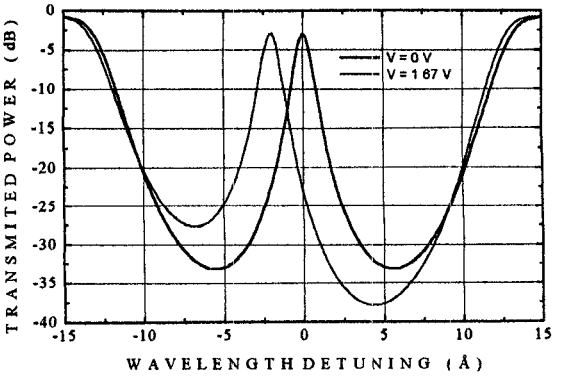

Figure 4. Power transmission spectra of the modulator with and without applied voltage.

region length yields smaller and wider-bandwidth devices, as can be observed in the figure.

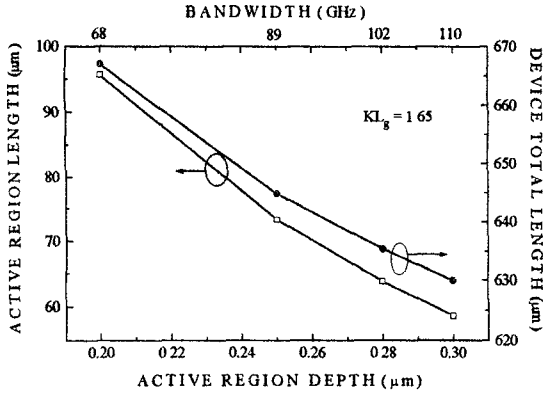

Figure 6. Device active region and total length as a function of the active region depth.

The extinction ratio and bandwidth as a function of the active region depth and KL_g as a parameter is shown in Figure 7. It can be seen in the figure, that higher extinction ratio at expense of the bandwidth is achieved with shallow active region and increased KL_g.

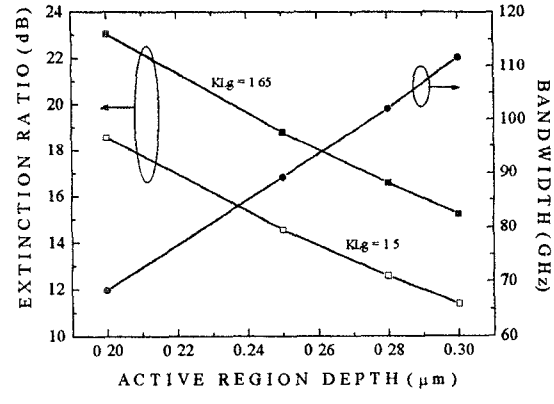

Figure 7. Device extinction ratio and bandwidth as a function of the active region depth.

The chirping parameter for electrorefraction modulators is defined as the ratio of refractive index to the extinction coefficient change, $\Delta n/\Delta k$, $\Delta k = (\lambda/4\pi)\,\Delta\alpha$, where $\Delta\alpha$ is the QCSE electroabsorption induced loss. As the QCSE in the CAQW is negligible $\Delta\alpha$ is also insignificant. Hence, the chirping parameter is very large and the modulator is chirp-free.

CONCLUSIONS

We proposed a wavelength-selective InGaAs/InP CAQW electrorefraction type optical intensity modulator operating at 1.55 μm. The device is based on a contradirectional exchange Bragg grating coupled-waveguide structure, which avoids the use of an interferometer. Simulations revealed that a non-optimized device 630 μm long presents a bandwidth of 111 GHz at 1.67 V, insertion loss of 3.18 dB, extinction ratio of 15.0 dB, and it is chirp-free. The modulator can also be optically tuned by providing ohmic contacts on the reflector sections. On the contrary of wavelength-selective single-waveguide devices, the input and output ports of this novel modulator are spatially separated which is attractive for monolithic integration with lasers, optical amplifiers, photodetectors etc. In addition, as the modulator is wavelength-selective it can be integrated in tandem for fabrication of compact multiplexed transmitters.

REFERENCES

1. J.E. Zucker, I. Bar-Joseph, BI Miller, U. Korean, and D.Sc. Chemical, "Quaternary Quantum Wells for Elector-Optic Intensity and Phase Modulation at 1.3 and 1.55 μm", Apple. Pays. Let., 54, 10, 1989.

2. C. Thirstrup, "Refractive Index Modulation Based on Excitonic Effects in GaInAs-InP Coupled Asymmetric Quantum Wells", IEEE J. Quantum Electron., 31, 988, 1995.

3.D. Marcuse, "Directional Couplers Made of Nonidentical Asymmetric Slabs. Part I: Synchronous Couplers", J. Lightwave Technol., 5, 113, 1987.

4. J. Hong and W Huang, "Coupled-Waveguide Exchange-Bragg Resonator Filters: Coupled-Mode Analysis with Loss and Gain", J. Lightwave Technol., 11, 226, 1993.

5. C.H. Henry, L.F. Johnson, R.A. Logan, and D.P. Clarke, "Determination of the Refractive Index of InGaAsP Epitaxial Layers by Mode Line Luminescence Spectroscopy", IEEE J. Quantum Electron., 21, 1887, 1985.

6. F. Fiedler and A. Schlachetzki, "Optical Parameters of InP Based Waveguides", Solid-State Electron., 30, 73, 1987.

7. J-P. Weber, "Optimization of the Carrier-Induced Effective Index Change in InGaAsP Waveguides - Applications to Tunable Bragg Filters", IEEE J. Quantum Electron., 30, 1801, 1994.

ACKNOWLEDGMENTS

The authors wish to thank the financial support of the National Council for Scientific and Technological Development (CNPq) Grant # 134.038/95-9.